

# SPECTRAL RATIO BIOSPHERIC LIDAR

Jonathan A. R. Rall<sup>(1)</sup> and Robert G. Knox<sup>(2)</sup>

<sup>(1)</sup>Laser Remote Sensing Branch Code 924 NASA Goddard Space Flight Center, Greenbelt, MD

[Jonathan.A.Rall@nasa.gov](mailto:Jonathan.A.Rall@nasa.gov)

<sup>(2)</sup>Biospheric Processes Branch Code 923 NASA Goddard Space Flight Center, Greenbelt, MD

[Robert.G.Knox@nasa.gov](mailto:Robert.G.Knox@nasa.gov)

## ABSTRACT

A new active vegetation index measurement technique has been developed and demonstrated using low power laser diodes to make horizontal-path lidar measurements of nearby deciduous foliage. The two wavelength laser transmitter operates within and adjacent to the 680 nm absorption feature exhibited by all chlorophyll containing vegetation. Measurements from early October through late November 2003 are presented and the results are discussed.

## 1. INTRODUCTION

The Normalized Difference Vegetation Index (NDVI) and related vegetation indices (VI) rely on the distinctive optical properties (reflectivity and absorption) of chlorophyll containing vegetation, Fig 1. The dominant pigment in plant leaves, Chl *a*, strongly absorbs visible light (from 0.4 to 0.7  $\mu\text{m}$ ) for use in photosynthesis, with blue and red peaks near 0.43 and 0.67  $\mu\text{m}$ . However, the cell structure of the leaves strongly reflects near-infrared light (from 0.7 to 1.2  $\mu\text{m}$ ). This transition around 0.7  $\mu\text{m}$  is referred to as the *red edge*. In general, if there is much less reflected radiation in red wavelengths than in near-infrared wavelengths, then the vegetation is likely healthy and dense whereas if there is little difference in the intensity of the reflected red and near-infrared wavelengths then plant leaves are likely sparse, absent, or dead.

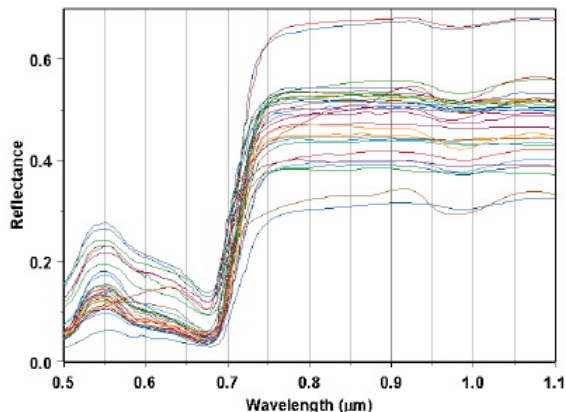


Fig. 1. Spectral Reflectance of Vegetation. [1]

A land-surface lidar that uses spectral reflectance to discriminate living vegetation from non-living sources of surface roughness would have great potential for airborne mapping and for future NASA missions. In particular, Earth-orbiting lidar missions to map biomass carbon and to measure dynamic topography and ecosystem change could yield much more accurate and specific data, if they include vertically-resolved discrimination of the types of surfaces measured. A lidar instrument that actively measures vegetation spectral response, in two narrow wavelength bands on either side of the *red edge* would also provide unprecedented information for calibration of passively acquired multi-spectral vegetation data (e.g. AVHRR). This is due to the precise pointing capability, narrow laser divergence (i.e., small spot size on the surface) and narrow fields of view possible with lidar instruments. Also, by keeping the two probe wavelengths close to the *red edge*, the lidar can measure and remove along-path reflectance from atmospheric aerosols. Therefore, any differences in measured spectral reflectance at the two probe wavelengths are due to differences in the surface features and not the atmospheric path. Precursor techniques used ratios of fundamental and frequency doubled Nd:YAG lidar signals (1064 & 532 nm, respectively) or active near-IR reflectance signals for target discrimination and ranging. Paired wavelengths near the vegetation *red edge* have not been used in existing lidar systems.

## 2. DEMONSTRATION SYSTEM

A low power demonstration instrument using two semiconductor laser diodes, a 20 cm diameter Schmidt-Cassegrain telescope, and two photon counting detectors was developed in the Laser Remote Sensing Branch of NASA's Goddard Space Flight Center. A block diagram of the instrument is shown in Fig. 2 and the specifications are listed in Table 1. Each laser beam is collimated, circularized, and expanded to ~40 mm diameter before being incoherently combined, i.e. near-fields & far-fields overlapped, using a mirror (M1) and dichroic filter (D1) as the combining element. Fine adjustments to the co-alignment of the two laser beams is done with

the Risley prisms (R1 & R2) whose angular deviation is demagnified by the beam expander ratios. The co-aligned beams are then boresighted with the telescope using two folding mirrors (M2 & M3). A video camera with a zoom lens is co-aligned with the instrument to ease pointing.

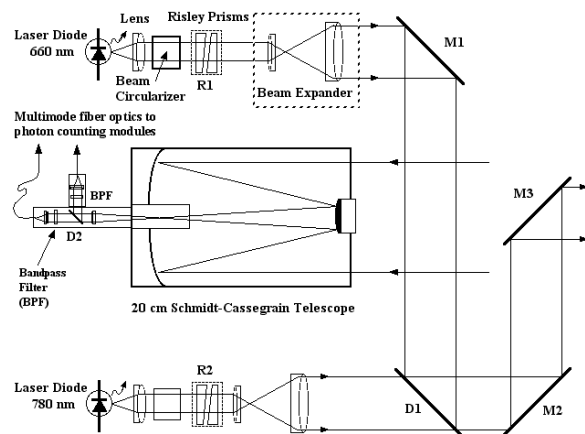


Fig. 2. Block Diagram of SRBL System

The backscattered light is collected by a 20 cm diameter Schmidt-Cassegrain telescope that has an adjustable iris at its focus to limit the receiver field of view (FOV). The light is recollimated after the field stop and split by a dichroic beam splitter into separate receiver paths. Each path has a narrow band optical filter and a focusing lens to couple the light into multimode fibers that couple the light into single photon counting modules (SPCM). The output pulses generated by each SPCM are collected by a multi-channel scalar, read-out and displayed on a desktop computer.



Fig. 3. SRBL demonstration instrument.

### 3. HORIZONTAL PATH MEASUREMENTS

This instrument was used during October and November 2003 to demonstrate the feasibility of the

underlying measurement concept, namely the ability to quantify the spectral reflectance of changing vegetation, i.e. deciduous trees changing color and dropping their foliage. The instrument was operated horizontally from a rooftop laboratory over several hundred meters to a stand of deciduous trees, Fig. 4. The laser diodes were synchronously pulsed with 100 ns wide pulses at 250 kHz pulse repetition frequency (PRF).

Table 1. Instrument Specifications

Item	Red	NIR
Laser Diode	Hitachi HL6501	Sanyo DL7140
Laser power	30 mW	70 mW
Wavelength	$660 \pm 5$ nm	$780 \pm 5$ nm
Beam splitter 45° Dichroic	$R > 95\%$ @ 658.5 nm, $T < 0.01\%$	$T > 90\%$ @ 781.0 nm
Telescope	20 cm Meade	20 cm Meade
Bandpass Filter	$658.5 \pm 0.1$ nm 0.30 nm FWHM	$781.0 \pm 0.2$ nm 0.26 nm FWHM
Detectors	SPCM-AQR-13-FC	SPCM-AQR-13-FC
Counters	Turbo MCS	Turbo MCS



Fig. 4. Stand of deciduous trees, target of measurements.

The average transmit power was 0.8 mW at 660 nm and 1.5 mW at 780 nm yielding pulse energies of 3.2 nJ and 6.0 nJ respectively. Initially, measurements were made to the side of a nearby building to normalize the data, i.e. correct for the difference in transmit powers between the red and NIR channels. The edge of the white-painted high bay of the building is visible in Fig 4. Data was acquired in two-second integrations, first from the building and then from the trees in the distance. Several measurements were made at different locations in the trees to average over different canopy surfaces that may include bark of tree trunks and branches as well as leaves. Figures 5 and 6 show the dramatic difference in reflectance of the foliage at the different wavelengths of incident light. The red signal in Fig.

5 is significantly attenuated while the NIR signal in Fig. 6 is strongly reflected. Both lasers have similar strength signals from the side of the building. Fig. 7 shows the ratio of NIR to Red signal scattered by the trees and building.

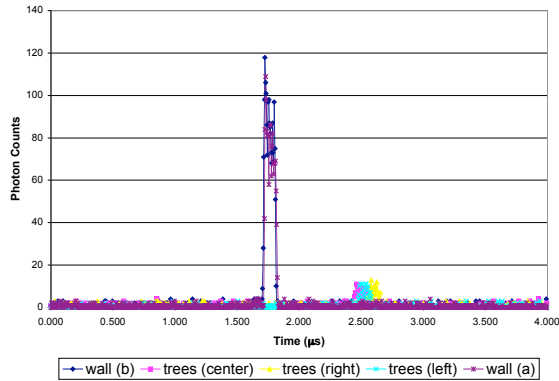


Fig. 5. Red channel, returns from wall & trees, October 10, 2003.

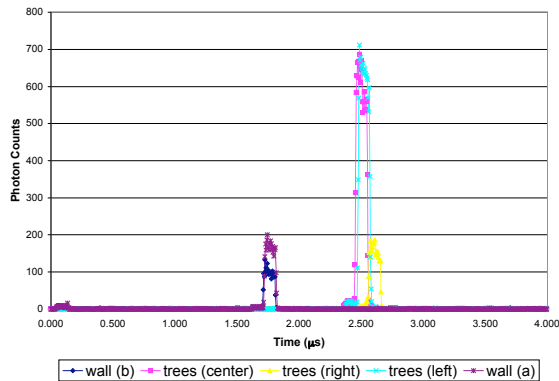


Fig. 6. NIR Channel, returns from wall & trees, October 10, 2003.

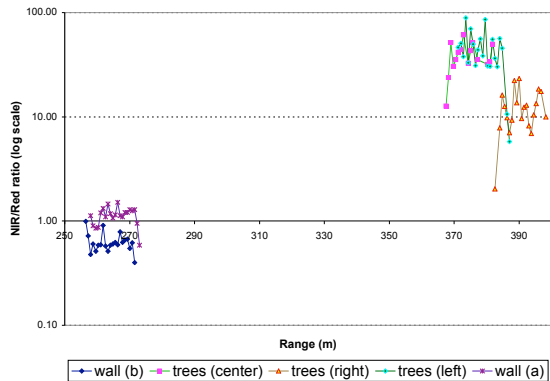


Fig. 7. The ratio of reflected NIR signal to the Red signal.

#### 4. INSTRUMENT CALIBRATION

To calibrate the instrument, that is to correct for differences in transmitter power and to understand

the receiver system response, measurements were made to a Spectralon® panel. Optical grade Spectralon® reflects more than 98% of incident light from the visible through near infrared and the reflectance varies less than 1% between 660 nm and 780 nm. A 25 cm square panel was set up on the roof of a nearby building, approximately 225 meters away. Data taken with the panel are shown in Fig 8. The ratio of the average reflectance between the red and NIR results in a system constant or normalization factor of approximately 4. This, in part, can be attributed to the factor of two difference in laser transmitter power with the additional factor of two due to the receiver response, e.g. gold coated mirrors in the telescope, alignment of aft optics, fiber optic coupling efficiency, etc. The large variance in the reflected signals from the reference panel is likely due to pointing jitter from the building vibrations, which caused the laser spots to dance on the surface of the panel. It is possible that the laser spots at times were on the edge of the panel possibly causing amplitude fluctuations. A larger Spectralon® panel will be used in the future to eliminate this error source and to better calibrate the system.

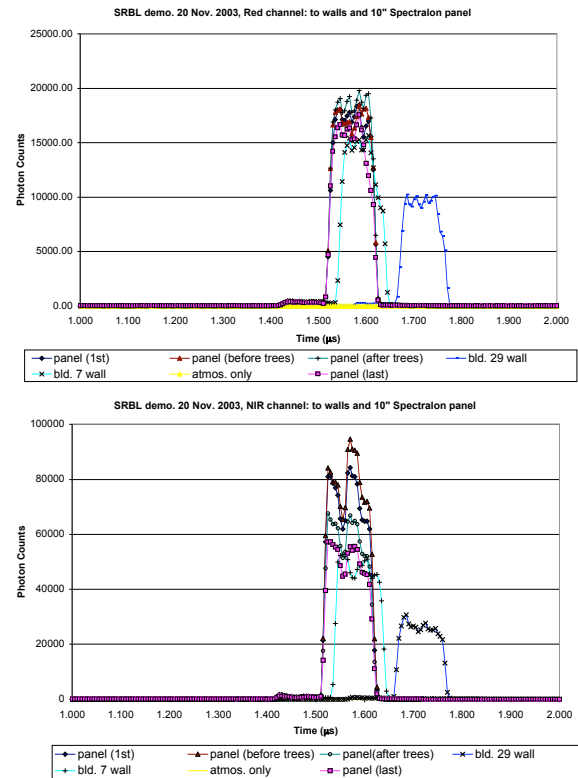


Fig. 8. System calibration measurements to reference panel.

#### 5. SPECTRAL REFLECTANCE OVER TIME

Measurements were made approximately once per week from October through November and are

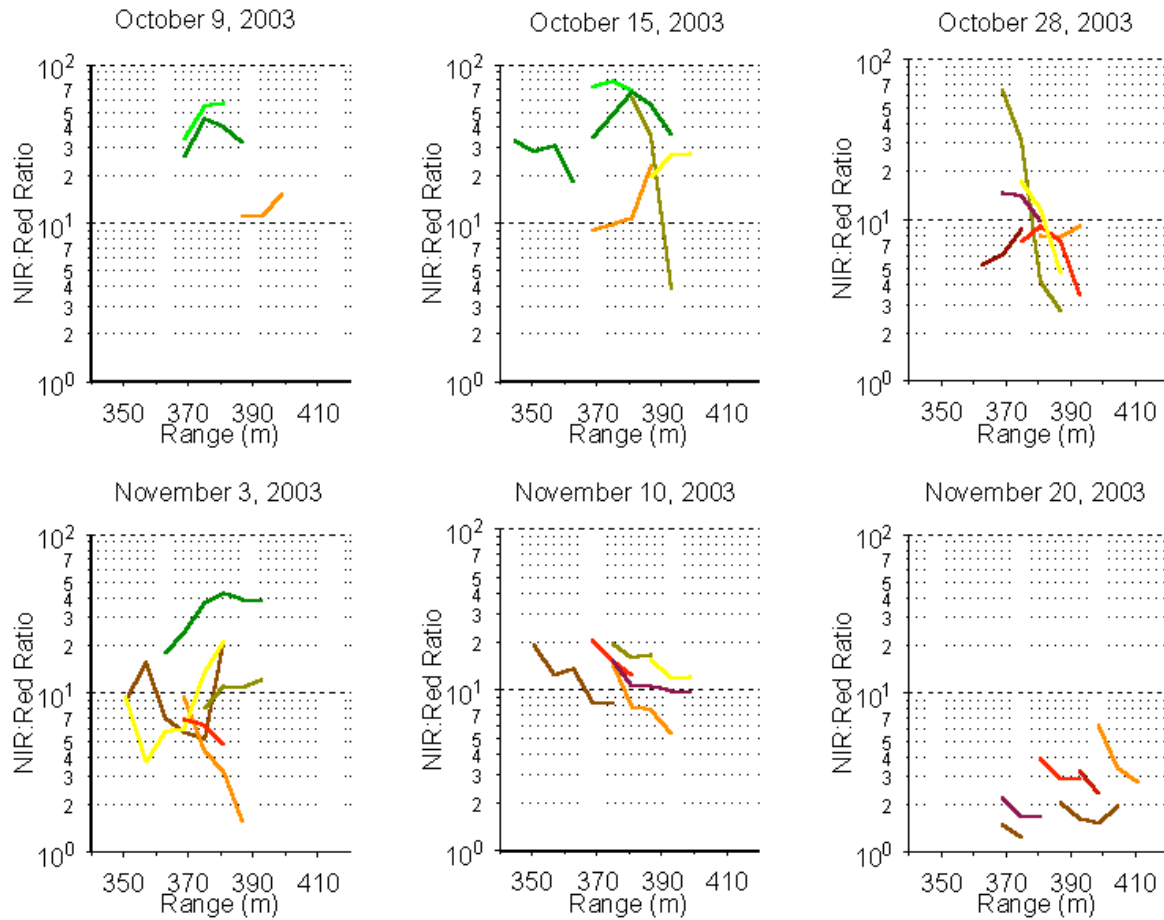


Fig. 9. Spectral reflectance ratios from October through November 2003.

shown in Fig 9. Since the collimated beam size at 350 meters is approximately 75 mm, multiple measurements to different trees and at different locations in the tree canopies were made. This reduced the possibility of hitting a single dead leaf in an otherwise healthy, dense canopy. Initial reflectance ratios of 40-50, indicating healthy, green vegetation, are evident from the measurements taken on October 9<sup>th</sup> and confirmed by their visual appearance in Fig 4. As time progresses and the vegetation loses chlorophyll content, the reflectance ratio drops and eventually settles at a ratio of 2-2.5 which is roughly equivalent to the ratio of the receiver system throughput for NIR/Red wavelengths.

## 6. CONCLUSIONS

We have successfully demonstrated a novel vegetation index lidar technique using two laser

diodes straddling the chlorophyll absorption peak at 680 nm. We have done an initial calibration of the system using a spectrally flat panel and made a time series measurement of spectral reflectance of deciduous trees as they changed color and dropped their leaves. We are developing higher power laser sources, based on frequency-doubled, rare-earth doped, fiber optic amplifiers to enable airborne and space borne, vertically resolved, vegetation index lidar measurements.

## 7. REFERENCES

- [1] Hall, F.G., K.F. Huemmrich, D.E. Strebel, S.J. Geotz, J.E. Nickeson, and K.D. Woods. 1992. Biophysical, Morphological, Canopy Optical Property, and Productivity Data From the Superior National Forest. NASA Technical Memorandum 104568.